Original Research

Glucocorticoid Alleviates Stress-induced Hypothalamic Nerve Injury by Inhibiting the GSDMD-dependent Pyroptosis Pathway

Shanyong Yi[1],*, Lijie Zhu[1], Yaxin Guo[1], Bin Zhao[1], Lai Wei[1], Zhijun Yao[2], Bin Yang[1,3],*

[1]Xinxiang Key Laboratory of Forensic Toxicology, School of Forensic Medicine, Xinxiang Medical University, 453003 Xinxiang, Henan, China
[2]School of Basic Medical Science, Xinxiang Medical University, 453003 Xinxiang, Henan, China
[3]The Second Affiliated Hospital of Xinxiang Medical University (Henan Mental Hospital), 453003 Xinxiang, Henan, China
*Correspondence: 201082@xxmu.edu.cn (Shanyong Yi); yangb257@163.com (Bin Yang)
Academic Editor: Bettina Platt

Abstract

Background: Excessive stress leads to stress injury but the underlying mechanism is not completely understood and current preventive protocols are inadequate. This study aimed to investigate if glucocorticoid (GC) reduces nerve damage in the hypothalamus caused by stress and to clarify the mechanisms involved. **Methods**: Behavioral alterations in stressed rats were observed using the open field test. Changes in the levels of stress hormones, inflammatory factors, and stress-related injury factors were detected using enzyme-linked immunosorbent assay (ELISA). Pathological alterations in the hypothalamus were observed using thionine staining and hematoxylin & eosin (HE) staining. The expression levels of proteins linked to pyroptosis were determined using western blotting. **Results**: Stressed rats presented obvious anxiety-like behavior; the levels of stress hormones, inflammatory factors, and injury-related factors fluctuated abnormally. Morphological findings indicated substantial damage in the hypothalamus. Stress-induced nerve injury was alleviated by low-dose GC treatment, which also dramatically decreased the concentrations of inflammation-associated markers and expression of the gasdermin D (GSDMD)-related pyroptosis pathway. **Conclusions**: Low-dose GC alleviates hypothalamic nerve injury by inhibiting the GSDMD-dependent pyroptosis pathway in stressed rats.

Keywords: glucocorticoid; stress; gasdermins; pyroptosis; hypothalamus

1. Introduction

As a systemic adaptation syndrome induced by various internal and external stimuli, stress faced by individuals cannot be ignored [1]. The effects of stress response include chemical reactions at the molecular level, regulation of the neuroendocrine system, and alterations in behavior, mood, and cognitive function [2]. Moderate stress activates the capacity of the organism to adapt to stress, while excessive stress may exceed the capacity of an organism to withstand stress, resulting in stress-induced injury [3,4]. Various adverse stress reactions lead to pathological changes in multiple systems and organs, which directly or indirectly lead to various diseases [5,6]. However, further exploration is needed to understand the characteristics and mechanism of stress-induced injury.

Pyroptosis is a recently identified gasdermins (GSDMs)-mediated programmed cell death [7]. As a protein superfamily, GSDMs are found only in vertebrates. The human GSDMs superfamily consists of the following members: Pejvakin (PJVK), gasdermin A (GSDMA), GSDMB, GSDMC, GSDMD, and GSDME [8,9]. The N-terminal (NT) domain of GSDMs, except PJVK, creatse membrane holes [10]. Under normal circumstances, with the autoinhibitory mechanism, the C-terminal (CT) domain and the NT pore-forming domain may combine to form a conserved two-domain structure, with the GSDM

proteins remaining inactive in the cytoplasm [11]. When GSDM-NT and GSDM-CT are separated because of abnormal circumstances, the self-inhibition vanishes [12]. After binding to a variety of lipids, GSDM-NT causes the cell membrane to form pore-like structures, which result in cell lysis, swelling, and the emission of substances that promote inflammation [13]. Previous studies by the current authors showed that stress leads to pathological changes such as cell swelling and disintegration in multiple brain regions of rats [14,15], but whether pyroptosis is involved in brain injury induced by stress and its detailed mechanism remains to be further explored.

When stimulated by various stress stimuli, the body secretes glucocorticoid (GC) in response to external stimuli [16]. GC enables the body to resist external factors by adjusting energy and metabolism [17]. Many studies have shown that GC is essential for lysosomal membrane integrity, anti-inflammatory and anti-shock mechanisms, and minimizing the damage caused by bacterial endotoxins [18,19]. However, chronic GC treatment leads to a variety of negative effects, such as brain inflammation and neurodegeneration [20], muscle atrophy, and osteonecrosis of the femoral head [21]. It has also been found that high dose or sustained usage of GC leads to muscle atrophy by inducing pyroptosis of muscle cells [22]. Unlike chronic GC treatment, it has been shown that low-dose GC effectively
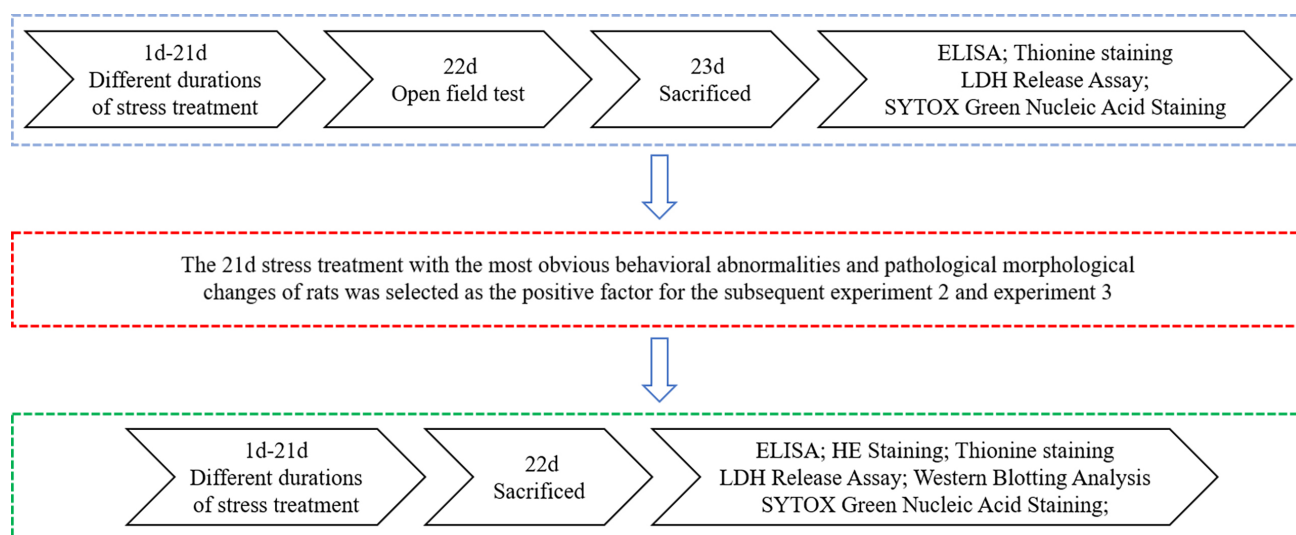
Fig. 1. Overall experimental flowchart. ELISA, enzyme-linked immunosorbent assay; LDH, Lactate dehydrogenase; HE Staining, Hematoxylin & eosin (HE) staining.

alleviates the negative effects of chronic stress, such as adaptive changes and depression-like behavior [23]. These results suggest that, unlike the side effects of high-dose GC, low-dose GC may have positive effects on a stressed organism. However, the protective mechanism of low-dose GC after stress, especially whether it might reduce stress-related nerve damage, should be investigated further.

Current research on stress has predominantly concentrated on peripheral organs or regions. Nevertheless, the impact of stress on the hypothalamus, which serves as the central regulatory hub for stress response, has largely been overlooked. For this reason, the current research concentrated on the hypothalamus, aiming to explore the mechanism behind stress-related nerve damage in this area and to establish a scientific foundation for preventing and treating stress-related injuries.

2. Materials and Methods

2.1 Animals

Adult male Sprague-Dawley (SD) rats, with an average weight of 200 ± 20 g, were procured from Beijing Vital River Laboratory Animal Technology Co., Ltd. (Beijing, China). The rats were housed under controlled conditions, which included a 12-hour light/dark cycle (with illumination commencing at 07:00), an ambient temperature maintained at 21 ± 2 °C, and a relative humidity of $50 \pm 5\%$. All subjects were provided with ad libitum access to food and water.

In Experiment 1, rats were distributed according to chance into six groups: control; 1 day of restraint stress combined with ice-water swimming (1 d RS + IS); 3 d RS + IS; 7 d RS + IS; 14 d RS + IS; and 21 d RS + IS (n = 10).

In Experiment 2, rats were distributed according to chance into four groups: control, 21 days of restraint

stress combined with ice-water swimming (stress), stress + Necrosulfonamide (stress + NSA, NSA: a GSDMD inhibitor), and NSA (n = 10).

In Experiment 3, rats were distributed according to chance into six groups: control (n = 12), 21 days of restraint stress combined with ice-water swimming (stress, n = 12), stress + GC (1 mg/kg) (n = 12), stress + GC (2 mg/kg) (n = 6), stress + GC (3 mg/kg) (n = 6), and GC (1 mg/kg) (n = 6). All the experimental procedures are shown in Fig. 1.

2.2 Animal Treatments

The stress treatment was carried out as previously described [14]. The rats were confined and couldn't move around freely (8:00 to 14:00) without food or water. Rats were then forced to swim for 5 min every day in frigid water. The duration of stress treatment was 1, 3, 7, 14, and 21 days. At the same time, control rats were deprived of food and water and kept in cages. The body weights of all rats were measured at 1, 3, 7, 14, and 21 days before modeling. We selected the 21-day stress group with notable pathological and behavioral alterations for mechanism study in follow-up experiment 2 and experiment 3.

In experiment 2, after 21 days of stress, the rats in the stress + NSA and NSA groups were injected intraperitoneally with 10 mg/kg of NSA (MCE, HY-100573, Monmouth Junction, NJ, USA; dissolved in 20% dimethyl sulfoxide (DMSO, MCE, HY-Y0320C)) at 08:00 for 7 days.

In experiment 3, after 21 days of stress, the rats in the stress + GC and GC groups were injected intraperitoneally with different concentrations of GC (Dexamethasone, a long-acting glucocorticoid, MCE, HY-14648, Monmouth Junction, NJ, USA; dissolved in normal saline) at 08:00 for 7 days.

2.3 Open Field Test

Open Field Test was conducted with SuperMaze (Shanghai, China). Rats were put into a square arena (0.9 m × 0.9 m × 0.3 m) that was split into sixteen squares of the same size on the second day after the stress treatment. Rats were let to explore freely for 5 min in the open field. A video camera was used to record the rats' movements. The core zone was defined as the four center squares, while the remaining squares were classified as the peripheral region. Following the testing, the quantity of rat feces was counted.

2.4 Tissue Preparation

Tissue handling followed established protocols [14]. On the second day after the open field test, 1% pentobarbital sodium (50 mg/kg, P3761, Sigma-Aldrich, St. Louis, MO, USA, in the vehicle: 0.9% saline) was administered intraperitoneally to anesthetize the rats. Then blood was extracted from the rats' abdominal aorta while rats were anesthetized. Subsequently, rats were executed by beheading. The brains were taken out and immediately preserved in 10% formalin (Sangon Biotech, A375256, Shanghai, China, in the vehicle: ddH$_2$O) for 48 hours. After being dehydrated by an ethanol series, paraffin was used to implant the fixed brains. Coronal sections were created using a stereotaxic atlas and a rotary microtome (RM2255, Leica, Shanghai, China) [24]. In successive 5-µm-thick coronal slices, the biggest hypothalamic areas were found, which corresponded to –3.0 mm from the bregma. The slices were examined under a light microscope (Olympus IX73, Olympus, Tokyo, Japan) after staining with thionine and hematoxylin & eosin (HE) staining.

2.5 Thionine Staining

Thionine staining was carried out as mentioned earlier [25]. Deparaffinized slices were immersed in a 4% thionine solution (Beyotime, Y267336, Shanghai, China, in the vehicle: ddH$_2$O) at 60 °C for 90 s. The slices were then mounted with neutral gum (Beyotime, C0173) after being dehydrated by an ethanol series.

2.6 HE Staining

HE staining was carried out as mentioned earlier [25]. The sections were first stained with hematoxylin (Beyotime, C0107) for 3 min, followed by immersion for 5 s in a solution of 1% hydrochloric acid alcohol. The sections were subsequently incubated with eosin (Beyotime, C0109) for 5 s. After being dehydrated by an ethanol series, the slices were then mounted with neutral gum (Beyotime, C0173).

2.7 Lactate Dehydrogenase (LDH) Release Assay

LDH level was detected with the LDH Assay kit (Solarbio Life Sciences, BC0685, Beijing, China). Moderate hypothalamic samples were homogenized with lactic dehydrogenase assay buffer, and the LDH test kit was used to treat the supernatants after they had been separated by centrifugation. Lastly, the colorimetric test was used to detect the treated samples at 450 nm (Multiskan MS photometer type 352, Labsystems, Helsinki, Finland).

2.8 SYTOX Green Nucleic Acid Staining (SYTOX)

Hypothalamic samples were sliced into tissue fragments, which were then carefully dissociated into individual cell solutions using Gentle MACS™ Dissociator (Miltenyi, Cologne, NRW, Germany). The individual cell solution was then resuspended with staining buffer and treated with SYTOX green nucleic acid staining solution (Invitrogen, S34860, Carlsbad, CA, USA) at room temperature without light. The number of SYTOX-positive cells was immediately analyzed with a flow cytometer (Beckman, Brea, CA, USA).

2.9 Enzyme-linked Immunosorbent Assay (ELISA)

The experimental procedure was carried out as mentioned earlier [14]. ELISA complete kits (USCN Life Science Inc., Wuhan, Hubei, China) were used to measure the levels of C-reactive protein (CRP, SEA821Ra), heat shock protein 70 (HSP70, SEA873Ra), GC (CEA540Ge), epinephrine (E, HEA858Ge), norepinephrine (NE, CEA907Ge), dopamine (DA, CEA851Ge), glucagon (Glu, CEB266Ra), angiotensin II (ANG II, CEA005Ra), interleukin-1β (IL-1β, SEA563Ra), and IL-18 (SEA064Ra). Blood was extracted from the rats' abdominal aorta while rats were anesthetized. After homogenizing the brain tissue, the supernatant was collected. After receiving the standard solution, serum and supernatant were incubated for 60 min at 37 °C. After adding horseradish peroxidase-labeled anti-rat CRP, HSP70, GC, E, NE, DA, Glu, ANG II, IL-1β, and IL-8 and melatonin secondary antibodies, the wells were incubated for 1.5 h at 37 °C. Following the removal of the liquid from the wells and three rounds of washing, color responses were produced using a tetramethylbenzidine color development solution. After 15 min without illumination and at room temperature, sulfuric acid (2 mmol/10 mL) was added. The plates were read using an ELISA reader (Multiskan MS photometer type 352, Labsystems, Helsinki, Finland) at 450 nm.

2.10 Western Blotting Analysis

Protein extracts (30 µg of protein/lane) from the hypothalamus were loaded onto SDS-PAGE gels (Beyotime, P0867M), separated by electrophoresis, and transferred to PVDF membranes (Beyotime, FFP26). After incubated overnight at 4 °C with rabbit GSDME-specific monoclonal antibody (1:2000, Abcam, ab215191, Cambridge, MA, USA), rabbit GSDMD-specific monoclonal antibody (1:1500, Abcam, ab219800), rabbit GSDMD-NT-specific monoclonal antibody (1:2000, Affinity Biosciences, DF13758, Cincinnati, OH, USA), rabbit cleaved-caspse-1-specific polyclonal antibody (1:1500, Affinity
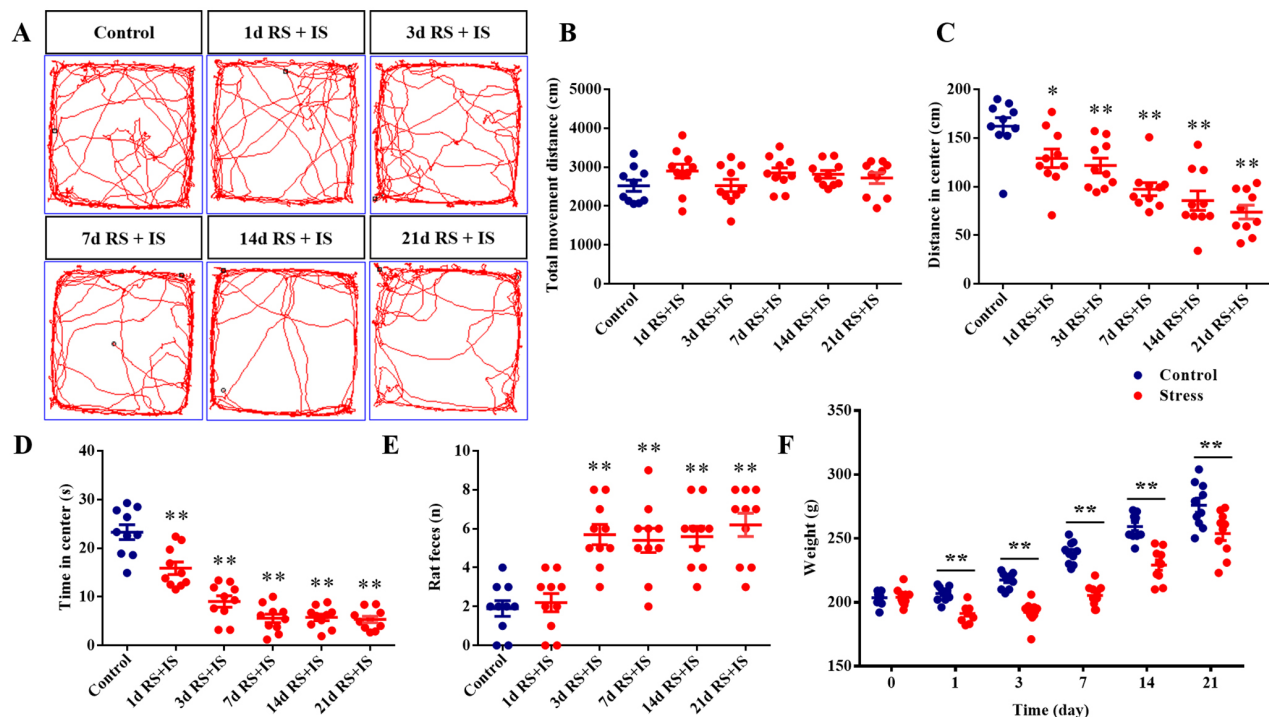
Fig. 2. Open-field test and body weight in Experiment 1 (n = 10). (A) The motion trajectory in the open field. (B) The movement distance in the open field. (C) The movement distance in the central area of the open field. (D) The cumulative duration in the central area of the open field. (E) The number of feces in the open field. (F) Body weight changes of stressed rats. The results are shown as the mean ± SEM, $^*p < 0.05$, $^{**}p < 0.01$ vs. the control group. d, day(s). RS + IS = restraint stress plus ice-water swimming.

Biosciences, AF4022), rabbit NLRP3-specific monoclonal antibody (1:1000, Abcam, ab263899), and mouse β-actin monoclonal antibody (1:2000, Beyotime, AF0003), the membranes were treated with horseradish peroxidase-conjugated goat anti-rabbit/mouse IgG (1:1000, Beyotime, A0208/A0216). Finally, the membranes were detected by an Odyssey gel imaging system (LI-COR, Inc., Lincoln, NE, USA).

2.11 Statistical Analysis

SPSS 21.0 (IBM Corp., Chicago, IL, USA) was used for statistical analysis. All data were found to be normally distributed by the Kolmogorov-Smirnov test ($p > 0.1$). The data are given as mean ± SEM. A post hoc least significant difference (LSD) t-test was used after the data had been analyzed using one-way or two-way ANOVA (as appropriate), to pinpoint particular group differences. $p < 0.05$ was the significant cutoff threshold.

3. Results

3.1 Stress Treatment Induced Abnormal Changes of Body Weight and Behavior in Rats

The behavioral changes in stressed rats were detected by open field test (Fig. 2A–E). ANOVA for the movement distance in the core region revealed significant differences [F (5, 54) = 15.03; $p < 0.0001$]. ANOVA for the cumu-

lative duration in the central area revealed significant differences [F (5, 54) = 45.67; $p < 0.0001$]. ANOVA for the number of feces in the open field revealed significant differences [F (5, 54) = 13.34; $p < 0.0001$]. Results revealed that after stress treatment, the cumulative duration and distance traveled in the core region dramatically dropped and the number of feces pellets significantly increased. Notably, these abnormal changes became more obvious with the extension of stress treatment. The present study also detected the effect of stress treatment on the body weight of rats (Fig. 2F). ANOVA for rat body weight revealed significant differences [F (5, 108) = 6.932; $p < 0.0001$]. Unlike those of normal rats, the weight gain of rats after stress treatment was significantly reduced. Even after short-term stress treatment, the body weight of rats showed a decreasing trend.

3.2 Stress Treatment Induced Dynamic Alterations of Stress-related Hormone Levels and Injury Factor Levels in Rat Serum

The levels of stress-related hormones were detected by ELISA (Fig. 3). ANOVAs for serum levels of GC, E, NE, DA, Glu and ANGII were found to be significantly different from control (respectively [F (5, 54) = 33.97; $p < 0.0001$], [F (5, 54) = 46.45; $p < 0.0001$], [F (5, 54) = 64.12; $p < 0.0001$], [F (5, 54) = 50.21; $p < 0.0001$], [F (5, 54) = 43.99; $p < 0.0001$], and [F (5, 54) = 112.2; $p < 0.0001$]). Results
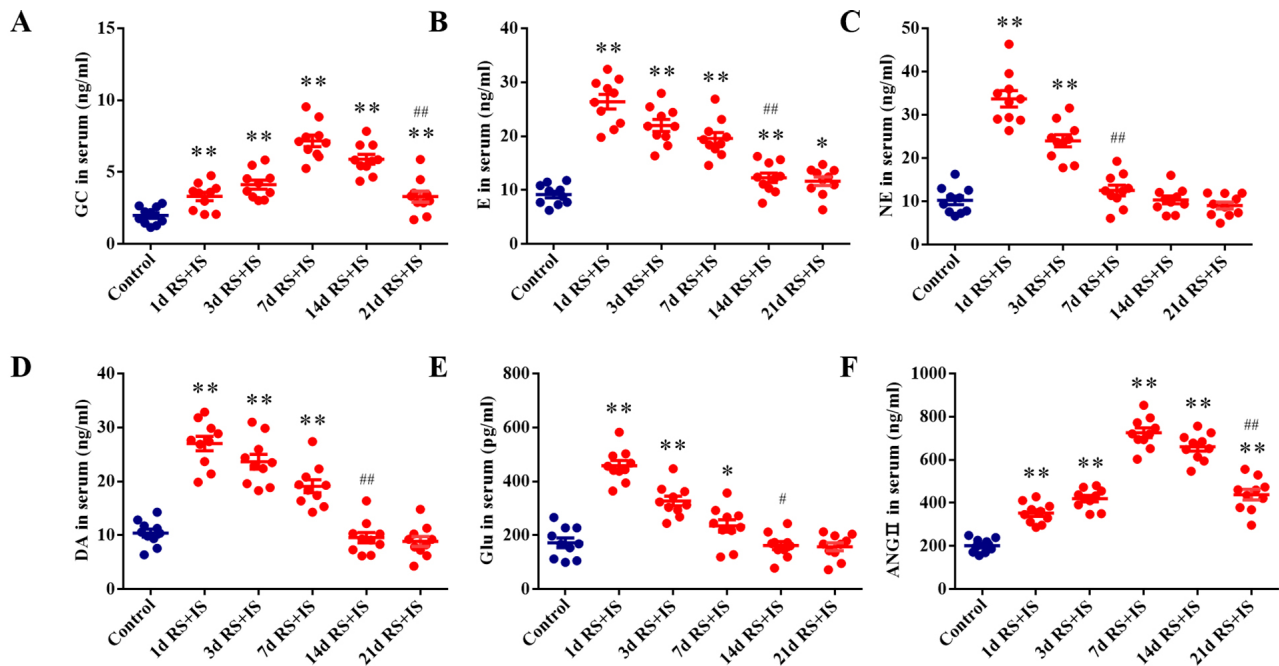
Fig. 3. Changes of stress-related hormone levels in Experiment 1 (n = 10). (A) The concentration of glucocorticoid (GC) in serum. (B) The concentration of epinephrine (E) in serum. (C) The concentration of norepinephrine (NE) in serum. (D) The concentration of dopamine (DA) in serum. (E) The concentration of glucagon (Glu) in serum. (F) The concentration of angiotensin II (ANG II) in serum. The results are shown as the mean $\pm$ SEM, $^*p < 0.05$, $^{**}p < 0.01$ vs. the control group, $^{##}p < 0.01$ vs. RS + IS group at 14 days in (A), $^{##}p < 0.01$ vs. RS + IS group at 7 days in (B), $^{##}p < 0.01$ vs. RS + IS group at 3 days in (C), $^{##}p < 0.01$ vs. RS + IS group at 7 days in (D), $^#p < 0.05$ vs. RS + IS group at 7 days in (E), $^{##}p < 0.01$ vs. RS + IS group at 14 days in (F). d, day(s). RS + IS = restraint stress plus ice-water swimming.
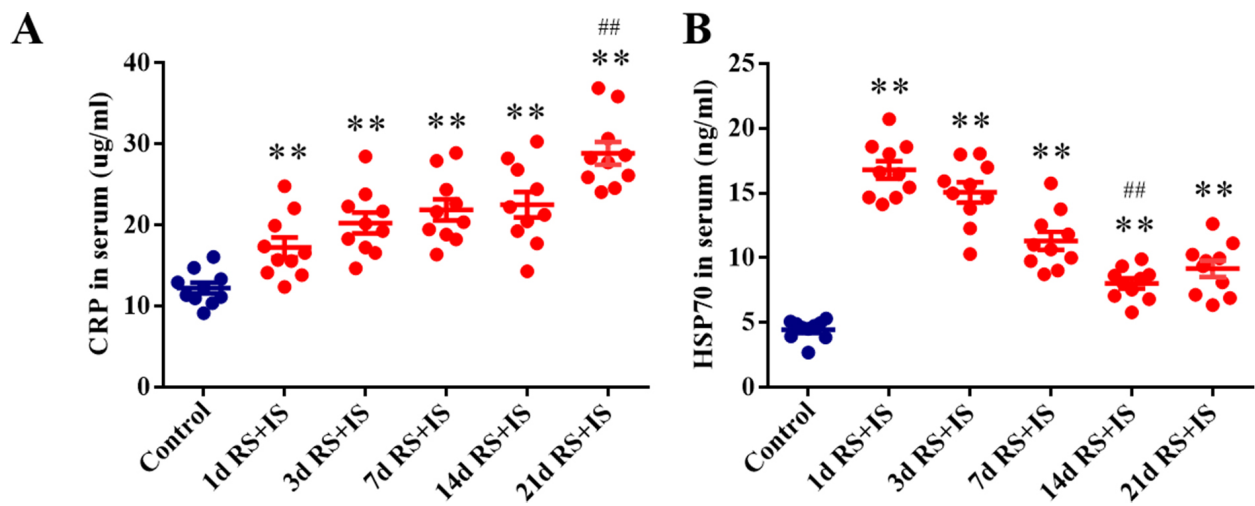

Fig. 4. Changes in the serum levels of C-reactive protein (CRP) and heat shock protein 70 (HSP70) in Experiment 1 (n = 10). (A) The concentration of CRP in serum. (B) The concentration of HSP70 in serum. The results are shown as the mean $\pm$ SEM, $^{**}p < 0.01$ vs. the control group, $^{##}p < 0.01$ vs. RS + IS group at 14 days in (A), $^{##}p < 0.01$ vs. RS + IS group at 7 days in (B). d, day(s). RS + IS = restraint stress plus ice-water swimming.

showed that after short-term stress treatment, the levels of GC, E, NE, DA, Glu, and ANG II were significantly increased in rat serum. However, with the extension of stress treatment, the levels of these hormones decreased significantly.

The current investigation found alterations in the concentrations of damage markers linked to stress (Fig. 4). ANOVAs for the serum level of CRP and HSP70 revealed significant differences (respectively, [$F_{(5, 54)} = 19.14$; $p < 0.0001$] and [$F_{(5, 54)} = 57.95$; $p < 0.0001$]). Results

revealed that, with the extension of stress treatment, the level of CRP showed a continuous upward trend; while the level of HSP70 reacted differently, as after short-term stress treatment, the level of HSP70 was significantly increased in rat serum. However, with the extension of stress treatment, the level of HSP70 decreased significantly.

3.3 Stress Treatment Induced Pathological Alterations and Inflammatory Responses in the Hypothalamus

Thionine staining detected pathological change (Fig. 5A). Pathological examination revealed that after short-term stress treatment, the cells in the hypothalamus showed no obvious histological changes; however, the number of abnormal neurons increased as the stress treatment was extended.

A lactate dehydrogenase (LDH) test determines the amount of cell content leakage. SYTOX Green is a green nucleic acid dye that easily passes through injured cell membranes, but not through the cell membrane of living cells. In the present study, LDH assay (Fig. 5B) and SYTOX green nucleic acid staining (Fig. 5C, **Supplementary Fig. 1A**) were conducted. ANOVAs for the release level of LDH and SYTOX revealed significant differences (respectively, [$F_{(5, 24)}$ = 12.27; $p < 0.0001$] and [$F_{(5, 24)}$ = 11.39; $p < 0.0001$]). Results revealed that after short-term stress treatment, the level of LDH leakage and the quantity of SYTOX green acid-positive cells in the hypothalamus showed no obvious change; however, with the extension of stress treatment, a continuous upward trend was revealed for both.

When pyroptosis occurs, cells with membrane pores release interleukin-1 beta (IL-1β) and IL-18, which induces local or systemic inflammation. The levels of IL-1β and IL-18 were detected by ELISA (Fig. 5D,E). ANOVAs for the levels of IL-1β in the hypothalamus revealed significant differences (respectively, [$F_{(5, 24)}$ = 9.608; $p < 0.0001$] and [$F_{(5, 24)}$ = 44.14; $p < 0.0001$]). Results showed that after short-term stress treatment, IL-1β and IL-18 levels showed no obvious change. However, with the extension of stress treatment, IL-1β and IL-18 levels increased.

3.4 GSDMD-related Pyroptosis Pathway Is Involved in Stress-related Pathological Alterations and Inflammatory Response

GSDMD and GSDME are well-known pyroptosis-related proteins. The expression status of GSDMD and GS-DME in the hypothalamus was detected by Western blot (Fig. 6A). Results revealed that the expression level of GS-DME in the hypothalamus was very low, but GSDMD was expressed abundantly. Necrosulfonamide (NSA) is a specific inhibitor of GSDMD that inhibits the cleavage of GS-DMD, oligomerization of GSDMD-NT, and membrane perforation. NSA was used to investigate the function of the GSDMD-associated pyroptosis pathway in stress-related hypothalamic damage. ANOVA for the level of GSDMD-NT in the hypothalamus revealed significant differences [$F_{(3, 20)}$ = 34.58; $p < 0.0001$]. Findings showed that stress dramatically increased the degree of GSDMD-NT in the hypothalamus and that NSA inhibited this effect (Fig. 6B,C). It is worth noting that NSA did not improve the behavioral abnormalities of stressed rats (**Supplementary Fig. 2**). All original WB images in Fig. 6A,B are provided in **Supplementary Material 1**.

Thionine staining detected pathological changes (Fig. 6D). Pathological findings revealed that NSA alleviated stress-induced hypothalamic injury. ANOVA for the release level of LDH, the quantity of SYTOX green acid positive cells and the levels of IL-1β and IL-18 in the hypothalamus revealed significant differences (respectively, [$F_{(3, 20)}$ = 23.46; $p < 0.0001$], [$F_{(3, 20)}$ = 15.76; $p < 0.0001$], [$F_{(3, 20)}$ = 23.65; $p < 0.0001$] and [$F_{(3, 20)}$ = 81.04; $p < 0.0001$]). Consistent with the above results, the LDH assay (Fig. 6E), SYTOX green nucleic acid staining (Fig. 6F, **Supplementary Fig. 1B**), and ELISA (Fig. 6G,H) revealed that NSA significantly relieved stress-induced pathological changes and inflammatory response.

3.5 Low-dose GC Dramatically Alleviated Stress-related Pathological Alterations and Inflammatory Response in the Hypothalamus via Inhibiting a GSDMD-dependent Pyroptosis Pathway

Pathological alterations were observed by Thionine staining (Fig. 7A) and hematoxylin and eosin staining (Fig. 7B). In contrast to higher-dose GC (2 mg/kg and 3 mg/kg) treatment, low-dose GC (1 mg/kg) significantly alleviated hypothalamic nerve damage. ANOVAs for the release level of LDH, the number of SYTOX green acid positive cells, and the level of IL-1β and IL-18 in the hypothalamus revealed significant differences (respectively, [$F_{(3, 20)}$ = 37.87; $p < 0.0001$], [$F_{(3, 20)}$ = 17.81; $p < 0.0001$], [$F_{(3, 20)}$ = 32.35; $p < 0.0001$] and [$F_{(3, 20)}$ = 69.55; $p < 0.0001$]). Changes in the LDH leakage (Fig. 7C), the number of SYTOX positive cells (Fig. 7D, **Supplementary Fig. 1C**), and the levels of IL-1β (Fig. 7E) and IL-18 (Fig. 7F) in the hypothalamus were also significantly reversed by low-dose GC. Expression levels of the GSDMD pyroptosis pathway (cleaved-caspase-1, NLRP3, and GSDMD-NT) were detected by Western blot (Fig. 8). ANOVAs for the level of cleaved-caspase-1, level of NLRP3 and GSDMD-NT in the hypothalamus revealed significant differences [$F_{(3, 20)}$ = 74.52; $p < 0.0001$], [$F_{(3, 20)}$ = 47.16; $p < 0.0001$] and [$F_{(3, 20)}$ = 23.59; $p < 0.0001$]). Consistent with the above results, low-dose GC significantly reversed the increased levels of GSDMD-related proteins induced by stress in the hypothalamus. All original WB images in Fig. 8A are provided in **Supplementary Material 2**.
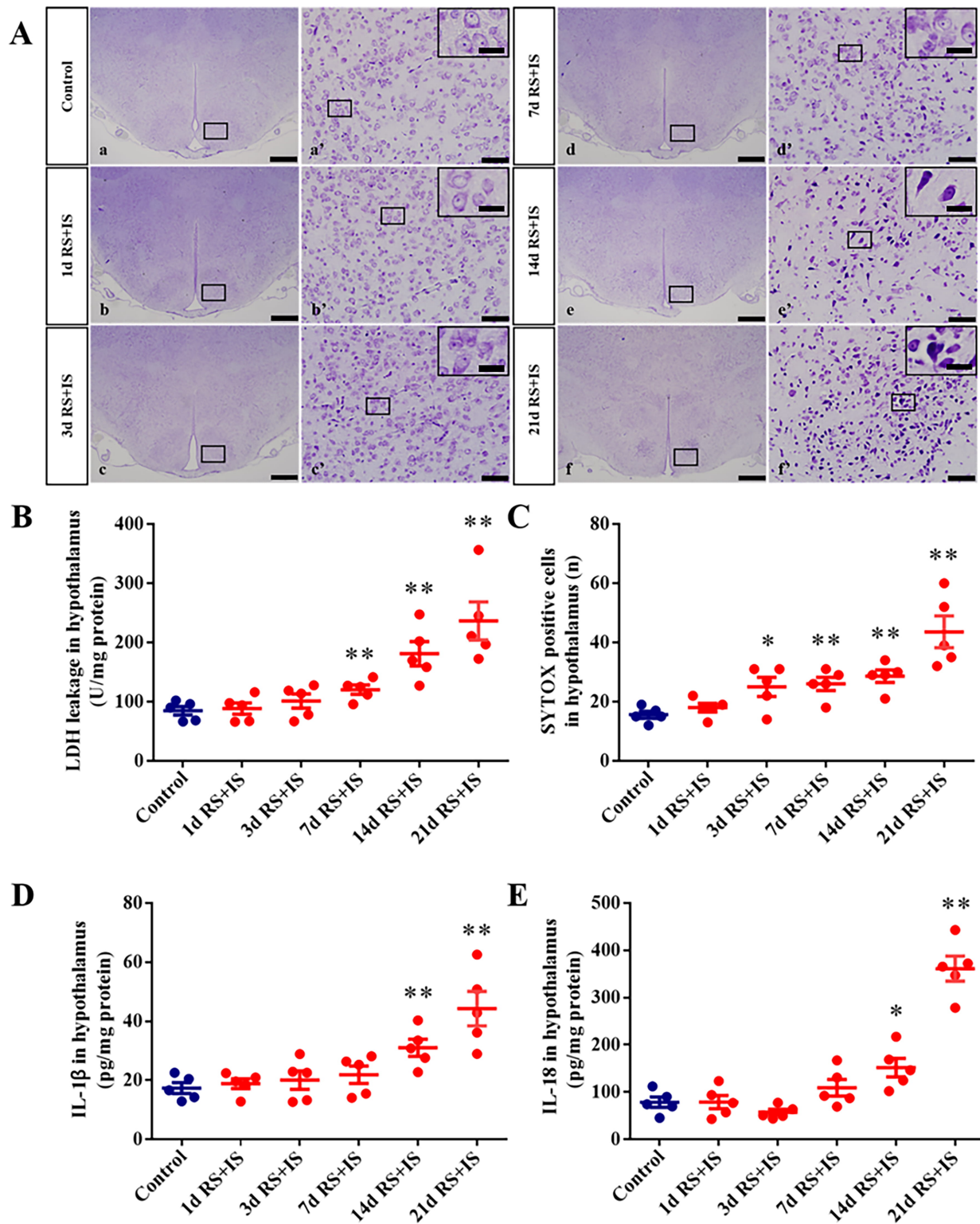
Fig. 5. Pathological changes in Experiment 1 (n = 5). (A) Pathological change in the hypothalamus, as shown by Thionine staining. (a'–f') are magnified areas of (a–f), high-power photomicrographs in the right corners of (a'–f') are enlarged from the rectangles in (a'–f'). (B) The lactate dehydrogenase (LDH) leakage in the hypothalamus. (C) The number of SYTOX green nucleic acid staining (SYTOX)-positive cells in the hypothalamus. (D) The level of interleukin-1β (IL-1β) in hypothalamus. (E) The level of IL-18 in the hypothalamus. (a–f) bars = 500 µm; (a'–f') bars = 50 µm; (high-power photomicrographs) bars = 15 µm. The results are shown as the mean $\pm$ SEM, $^*p < 0.05$, $^{**}p < 0.01$ vs. the control group. d, day(s). RS + IS = restraint stress plus ice-water swimming.
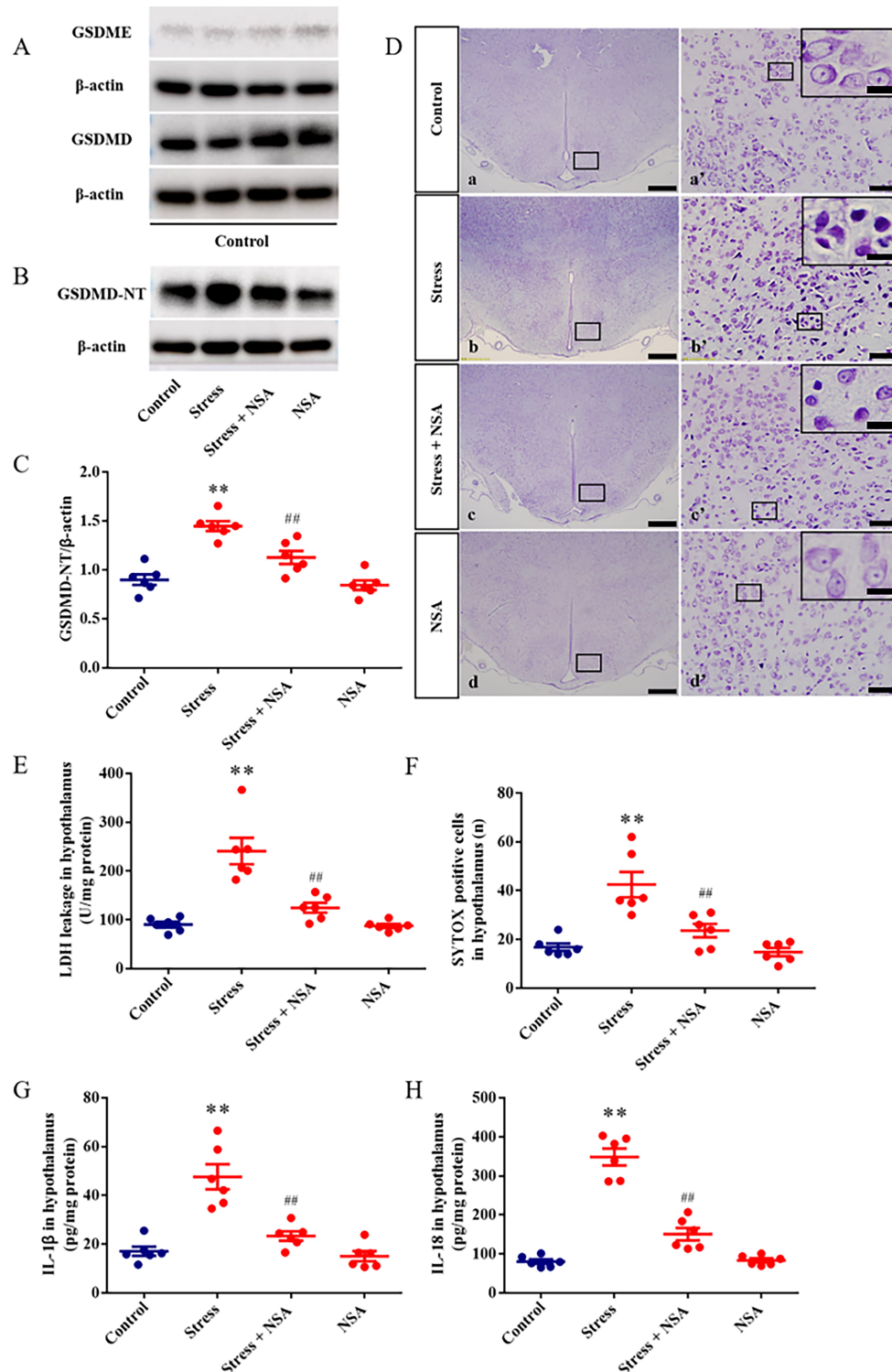
Fig. 6. Pyroptosis-related protein levels and pathological alterations in the hypothalamus in Experiment 2. (A) Representative blots showing the expression of gasdermin E (GSDME) (n = 6) and GSDMD (n = 6). (B) Representative blot showing the expression of GSDMD-N-terminal (GSDMD-NT) (n = 6). (C) Relative protein expression level of GSDMD-NT. (D) Pathological alterations in the hypothalamus, as shown by Thionine staining. (a'–d') are magnified areas of (a–d), high-power photomicrographs in the right corners of (a'–d') are enlarged from the rectangles in (a'–d'). (E) The LDH leakage in the hypothalamus. (F) The number of SYTOX-positive cells in the hypothalamus. (G) The level of IL-1β in the hypothalamus. (H) The level of IL-18 in the hypothalamus. (a–d) bars = 500 μm; (a'–d') bars = 50 μm; (high-power photomicrographs) bars = 15 μm. The results are shown as the mean ± SEM, $^{**}p < 0.01$ vs. the control group, $^{##}p < 0.01$ vs. the stress group. NSA: Necrosulfonamide, GSDMD inhibitor.
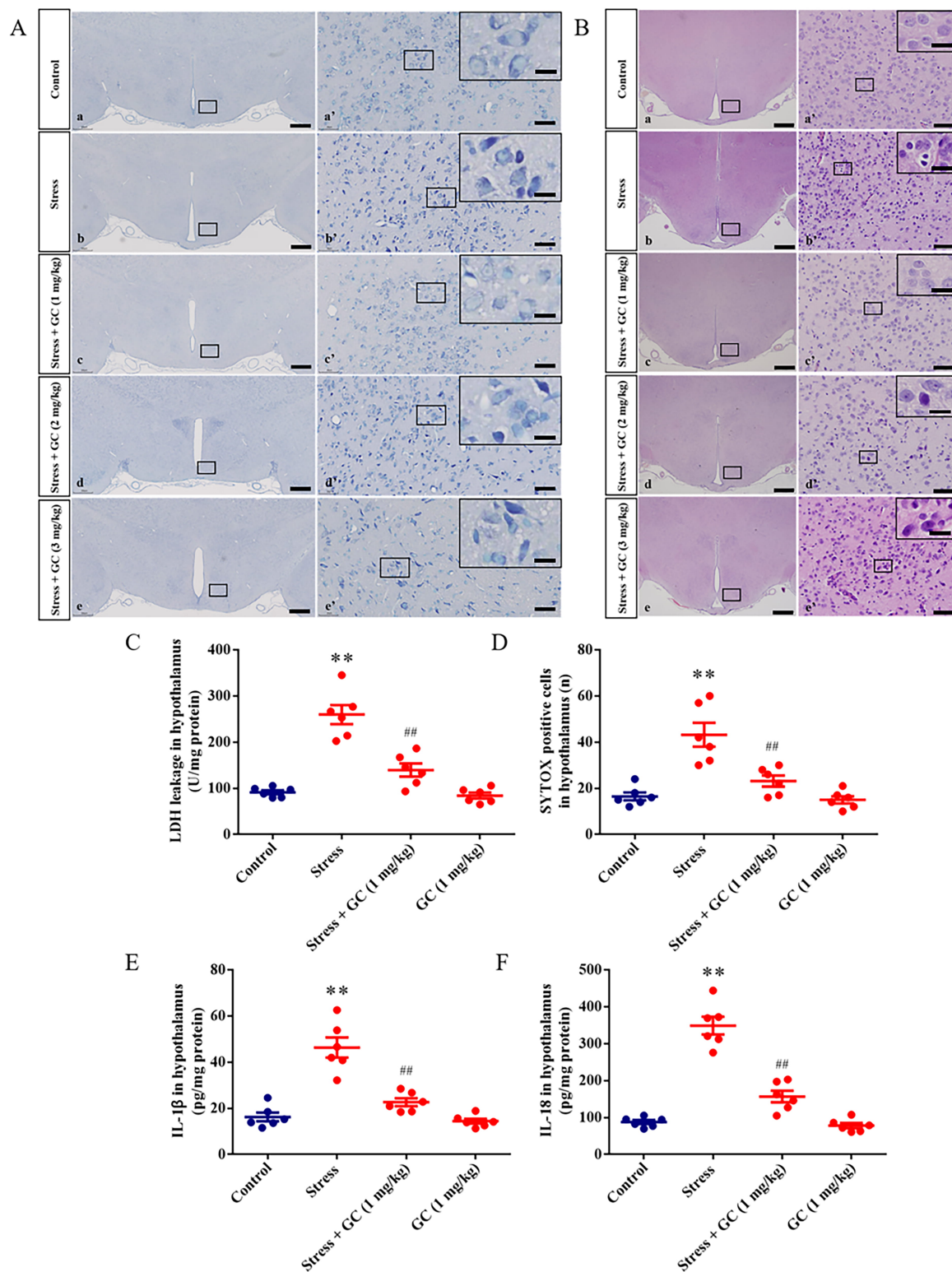
Fig. 7. Pathological changes in Experiment 3 (n = 6). (A) Pathological changes in the hypothalamus, as shown by Thionine staining. (a'–e') are magnified areas of (a–e), high-power photomicrographs in the right corners of (a'–e') are enlarged from the rectangles in (a'–e'). (B) Pathological changes in the hypothalamus, as shown by HE staining. (a'–e') are magnified areas of (a–e), high-power photomicrographs in the right corners of (a'–e') are enlarged from the rectangles in (a'–e'). (C) The LDH leakage in the hypothalamus. (D) The number of SYTOX-positive cells in the hypothalamus. (E) The level of IL-1β in the hypothalamus. (F) The level of IL-18 in the hypothalamus. (a–e) bars = 500 μm; (a'–e') bars = 50 μm; (high-power photomicrographs) bars = 15 μm. The results are shown as the mean ± SEM, $^{**}p < 0.01$ vs. the control group, $^{##}p < 0.01$ vs. the stress group.
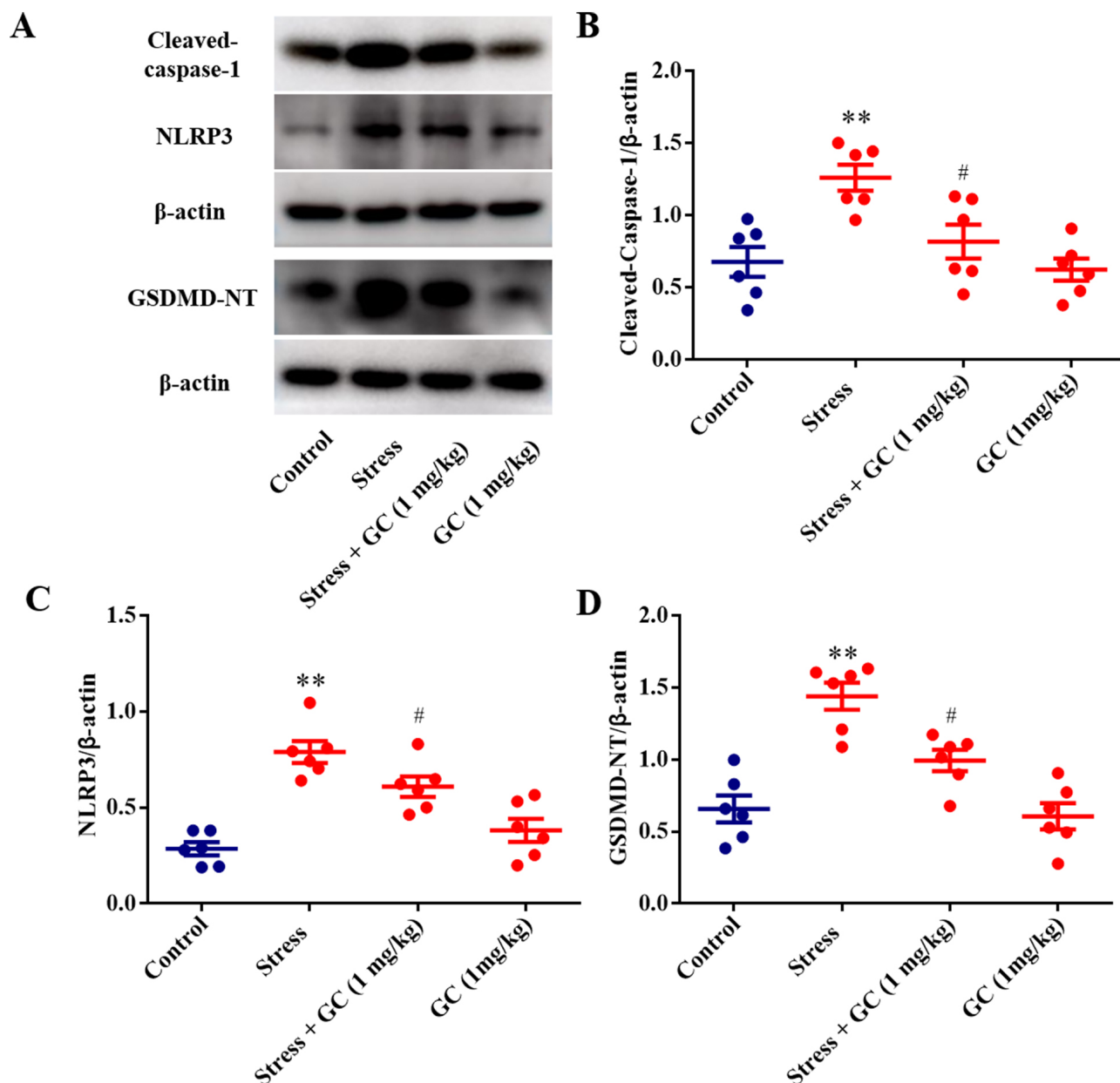
Fig. 8. The expression levels of Cleaved-cysteinyl aspartate specific proteinase-1 (Cleaved-caspase-1), nucleotide-binding oligomerization domain-like receptor protein 3 (NLRP3), and GSDMD-NT in the hypothalamus in Experiment 3 (n = 6). (A) Representative blots showing the expression of Cleaved-caspase-1, NLRP3, and GSDMD-NT. (B) Relative protein expression level of Cleaved-caspase-1. (C) Relative protein expression level of NLRP3. (D) Relative protein expression level of GSDMD-NT. The results are shown as the mean $\pm$ SEM, $^{**}p < 0.01$ vs. the control group, $^{\#}p < 0.05$ vs. the stress group. GC, glucocorticoid.

4. Discussion

The current research aimed to investigate how complicated psychosomatic stress affects the structure and function of the brain, as well as to identify protective measures for stress-induced injury. To achieve this goal, a combined stress rat model was reproduced via restraint plus ice water swimming, as described in a previous study [26]. Previous research has indicated that the anomalous anxiety and depression behavior of rats can be utilized to assess the effective replication of stress models [27,28]. In research

by the current authors, the behavioral findings showed that the number of feces pellets of stressed rats significantly increased with prolonged stress and that in the core location, the movement distance and cumulative duration were greatly decreased. These findings suggested that stressed rats exhibit clear anxiety-like behavior. Additionally, normal rats continued to gain weight with prolonged stress, whereas the weight of stressed rats initially showed a slight decrease during the early stages of stress, followed by a slowly increasing trend of weight gain over time. These ab-

normal changes in body weight and behavior showed that the rats were under a great deal of physiological and psychological stress, validating that the stress paradigm was successfully replicated.

Stress triggers systemic endocrine responses, and the hypothalamic–pituitary–adrenal (HPA) axis and the sympathetic adrenomedullary (SA) system play central roles in the stress response [29]. The activated HPA axis promotes the secretion of GC, whereas the excited SA system promotes the secretion of catecholamines E, NE, and DA. The increased secretion of GC, DA, E, and NE helps regulate energy and metabolism, thereby enhancing resistance to external risk factors [30]. Current research indicates that the increased secretion of glucagon (Glu) under stress conditions mobilizes the body's energy reserves to cope with stress stimuli [31]. Several studies have demonstrated that angiotensin II (ANG II) protects the stressed rat brain [32,33]. In short, changes in the levels of GC, E, NE, DA, Glu, and Ang II reflect the stress intensity experienced by the body. In the present study, those levels were significantly increased in the serum of rats exposed to short-term stress treatment, which might enhance the capacity to withstand stress stimuli. However, with the extension of stress treatment, the serum concentrations of NE, DA, and Glu returned to normal levels and although the levels of serum GC, E, and Ang II in stressed rats remained higher than those in normal rats, the relevant values continued to decrease. Such results suggest that short-term stress treatment upregulates the expression of stress hormones, which might improve the ability of the body to cope with stress; however, long-term stress treatment leads to endocrine disorders and diminished protective effects. This is consistent with previous study, as when stress becomes too severe or persists for too long, its intensity exceeds the body's self-regulatory ability [34], suggesting that long-term stress in the present study might lead to body injury and dysfunction.

C-reactive protein (CRP) levels in the blood increase significantly in response to infection or injury [35]. According to a prior study, chronic stress has been linked to an elevated level of blood CRP [36]. In the current research, stressed rats presented a continuous increase in the serum level of CRP, suggesting that long-term stress might lead to evident injury and inflammatory response.

To sustain cell life, Heat shock proteins (HSPs) perform several vital physiological tasks inside cells and are critical to the synergy of immunological activity [37]. Under stress conditions, the expression level of HSP70 is rapidly upregulated, which helps to mitigate the progression of the stress response [38]. In the study reported here, stressed rats presented a consistently high level of serum HSP70; however, with prolonged stress, the level of HSP70 significantly decreased, indicating that long-term stress surpassed the adaptive capacity of the body, which might lead to body injury and dysfunction.

In the present study, morphological results were consistent with the changes in stress hormones and injury factors. Thionine staining showed that long-term stress caused tissue edema, cell pyknosis, and significant microglial proliferation in the hypothalamus; the amount of LDH leakage, SYTOX-positive cells, and interleukin-1β (IL-1β) and IL-18 levels in the hypothalamus all steadily increased over time. This showed that pyroptosis-related pathological alterations in the hypothalamus were brought on by prolonged stress, indicating that pyroptosis could play a role in the process of hypothalamic damage in stressed rats.

The current study revealed six subtypes of GSDMs, of which GSDMD and GSDME are the main types in the nervous system [39]. In the present study, the expression level of GSDME in the hypothalamus was very low, but GSDMD was expressed abundantly. As a GSDMD inhibitor, NSA significantly inhibited the increase in GSDMD-NT level and alleviated the degree of prolonged stress-related hypothalamic nerve damage; NSA also alleviated pyroptosis-related alterations, such as LDH leakage, SYTOX positive cells, and IL-1β and IL-18 levels. These findings suggested that the GSDMD-dependent pyroptosis pathway was associated with stress-induced hypothalamic damage.

Previous research has shown that a high serum GC level has the ability to penetrate the blood-brain barrier and cause nerve damage [40], which suggests that the sustained high level of GC in the present study may be an important factor in long-term stress-induced hypothalamic injury. However, other research shows that low-dose GC effectively reduces the detrimental consequences of chronic stress, including adaptive modifications [23], which implies that appropriate GC treatment after long-term stress reduces its negative effects. However, whether GC treatment alleviates neurological injury induced by long-term stress and the detailed mechanism by which it occurs, should be investigated further. In the current research, as opposed to higher-dose GC treatment, low-dose GC significantly reduced stress-related hypothalamic damage; related changes in the LDH leakage, the number of SYTOX-positive cells, and the levels of IL-1β and IL-18 in the hypothalamus were also significantly reversed by low-dose GC. These results suggested that administration of low-dose GC markedly reduced pyroptosis-associated nerve damage in the hypothalamus of stressed rats.

As an important role of the nucleotide-binding oligomerization domain-like receptor family, nucleotide-binding oligomerization domain-like receptor protein 3 (NLRP3) is one of the cores of innate immunity [41]. The activated NLRP3 inflammasome promotes the activation of the precursor of intracellular IL-1β by activating cysteinyl aspartate specific proteinase-1 (caspase-1) and forming cleaved-caspase-1, which causes pyroptosis by activating GSDMD [42]. In this research, the levels of cleaved-caspase-1, NLRP3, and GSDMD-NT were markedly elevated in stressed rats, but low-dose GC treatment sig-

nificantly inhibited the expression of cleaved-caspase-1, NLRP3, and GSDMD-NT. The above findings suggested that low-dose GC treatment reduced the level of NLRP3 and then restrained the formation of the NLRP3 inflammasome, which inhibited the activation of caspase-1, and ultimately inhibited the formation of GSDMD-NT. In summary, these findings indicated that low-dose GC treatment alleviates the activation degree of the GSDMD-related pyroptosis pathway in stressed rats. In contrast to high-level GC, which can directly cross the blood-brain barrier and induce neural damage, and unlike high-dose GC treatment after stress, which fails to alleviate pyroptosis-associated neural injury, we propose that low-dose GC treatment after stress may reverse stress-induced detrimental gene expression patterns, thereby ameliorating stress-mediated neural injury and adaptive maladjustments. However, the underlying mechanism still requires further in-depth investigation to provide robust scientific substantiation.

5. Conclusions

In conclusion, pyroptosis is a contributing mechanism of stress-related hypothalamus injury and low-dose GC alleviates stress-related hypothalamic nerve damage by inhibiting the GSDMD-dependent pyroptosis pathway. The authors believe that this study provides a new perspective for future research on stress-induced nerve injury.

6. Limitations

The present study has several limitations, which also represent directions for our future research. First, we did not perform cellular experiments to further elucidate the underlying injury mechanism. Second, the detailed mechanism by which GC suppresses GSDMD-dependent pyroptosis remains to be fully investigated.

Availability of Data and Materials

Data will be made available on request.

Author Contributions

SY, LZ, YG, LW, BZ, and ZY performed experiments. SY created all figures. SY and BY conceived the project and wrote the manuscript. All authors contributed to editorial changes in the manuscript. All authors read and approved the final manuscript. All authors have participated sufficiently in the work and agreed to be accountable for all aspects of the work.

Ethics Approval and Consent to Participate

The research protocol was approved by the Animal Care and Use Committee of Xinxiang Medical University (Ethic Approval Number: AE-2022-09/04) and the animals were cared for in accordance with the National Institutes of Health Guide for the Care and Use of Laboratory Animals.

Conflict of Interest

The authors declare no conflict of interest.

Supplementary Material

Supplementary material associated with this article can be found, in the online version, at https://doi.org/10.31083/JIN39532.

References

[1] Reser JE. Chronic stress, cortical plasticity and neuroecology. Behavioural Processes. 2016; 129: 105–115. https://doi.org/10.1016/j.beproc.2016.06.010.

[2] Galluzzi L, Yamazaki T, Kroemer G. Linking cellular stress responses to systemic homeostasis. Nature Reviews. Molecular Cell Biology. 2018; 19: 731–745. https://doi.org/10.1038/s41580-018-0068-0.

[3] Bienertova-Vasku J, Lenart P, Scheringer M. Eustress and Distress: Neither Good Nor Bad, but Rather the Same? BioEssays: News and Reviews in Molecular, Cellular and Developmental Biology. 2020; 42: e1900238. https://doi.org/10.1002/bies.201900238.

[4] Parker KN, Ragsdale JM. Effects of Distress and Eustress on Changes in Fatigue from Waking to Working. Applied Psychology. Health and Well-being. 2015; 7: 293–315. https://doi.org/10.1111/aphw.12049.

[5] van Dokkum NH, de Kroon MLA, Reijneveld SA, Bos AF. Neonatal Stress, Health, and Development in Preterms: A Systematic Review. Pediatrics. 2021; 148: e2021050414. https://doi.org/10.1542/peds.2021-050414.

[6] Yaribeygi H, Panahi Y, Sahraei H, Johnston TP, Sahebkar A. The impact of stress on body function: A review. EXCLI Journal. 2017; 16: 1057–1072. https://doi.org/10.17179/excli2017-480.

[7] Wei Y, Yang L, Pandeya A, Cui J, Zhang Y, Li Z. Pyroptosis-Induced Inflammation and Tissue Damage. Journal of Molecular Biology. 2022; 434: 167301. https://doi.org/10.1016/j.jmb.2021.167301.

[8] Feng S, Fox D, Man SM. Mechanisms of Gasdermin Family Members in Inflammasome Signaling and Cell Death. Journal of Molecular Biology. 2018; 430: 3068–3080. https://doi.org/10.1016/j.jmb.2018.07.002.

[9] Kovacs SB, Miao EA. Gasdermins: Effectors of Pyroptosis. Trends in Cell Biology. 2017; 27: 673–684. https://doi.org/10.1016/j.tcb.2017.05.005.

[10] Ding J, Wang K, Liu W, She Y, Sun Q, Shi J, et al. Pore-forming activity and structural autoinhibition of the gasdermin family. Nature. 2016; 535: 111–116. https://doi.org/10.1038/nature18590.

[11] Shi J, Zhao Y, Wang K, Shi X, Wang Y, Huang H, et al. Cleavage of GSDMD by inflammatory caspases determines pyroptotic cell death. Nature. 2015; 526: 660–665. https://doi.org/10.1038/nature15514.

[12] Broz P, Pelegrín P, Shao F. The gasdermins, a protein family executing cell death and inflammation. Nature Reviews. Immunology. 2020; 20: 143–157. https://doi.org/10.1038/s41577-019-0228-2.

IMR Press

[13] Tsuchiya K. Switching from Apoptosis to Pyroptosis: Gasdermin-Elicited Inflammation and Antitumor Immunity. International Journal of Molecular Sciences. 2021; 22: 426. https://doi.org/10.3390/ijms22010426.

[14] Yi S, Shi W, Wang H, Ma C, Zhang X, Wang S, *et al*. Endoplasmic Reticulum Stress PERK-ATF4-CHOP Pathway Is Associated with Hypothalamic Neuronal Injury in Different Durations of Stress in Rats. Frontiers in Neuroscience. 2017; 11: 152. https://doi.org/10.3389/fnins.2017.00152.

[15] Hao R, Gao X, Lu Q, Zhao T, Lu X, Zhang F, *et al*. CUMS induces depressive-like behaviors and cognition impairment by activating the ERS-NLRP3 signaling pathway in mice. Journal of affective disorders. 2025; 369: 547–558. https://doi.org/10.1016/j.jad.2024.10.001.

[16] Halabicky OM, Giang CW, Miller AL, Peterson KE. Lead exposure, glucocorticoids, and physiological stress across the life course: A systematic review. Environmental Pollution (Barking, Essex: 1987). 2024; 345: 123329. https://doi.org/10.1016/j.envpol.2024.123329.

[17] Lehmann M, Haury K, Oster H, Astiz M. Circadian glucocorticoids throughout development. Frontiers in Neuroscience. 2023; 17: 1165230. https://doi.org/10.3389/fnins.2023.1165230.

[18] Liu B, Zhang TN, Knight JK, Goodwin JE. The Glucocorticoid Receptor in Cardiovascular Health and Disease. Cells. 2019; 8: 1227. https://doi.org/10.3390/cells8101227.

[19] Kasahara E, Sekiyama A, Hori M, Kuratsune D, Fujisawa N, Chida D, *et al*. Stress-Induced Glucocorticoid Release Upregulates Uncoupling Protein-2 Expression and Enhances Resistance to Endotoxin-Induced Lethality. Neuroimmunomodulation. 2015; 22: 279–292. https://doi.org/10.1159/000368802.

[20] Hu W, Zhang Y, Wu W, Yin Y, Huang D, Wang Y, *et al*. Chronic glucocorticoids exposure enhances neurodegeneration in the frontal cortex and hippocampus via NLRP-1 inflammasome activation in male mice. Brain, Behavior, and Immunity. 2016; 52: 58–70. https://doi.org/10.1016/j.bbi.2015.09.019.

[21] Hu K, Adachi JD. Glucocorticoid induced osteoporosis. Expert Review of Endocrinology & Metabolism. 2019; 14: 259–266. https://doi.org/10.1080/17446651.2019.1617131.

[22] Wang L, Jiao XF, Wu C, Li XQ, Sun HX, Shen XY, *et al*. Trimetazidine attenuates dexamethasone-induced muscle atrophy via inhibiting NLRP3/GSDMD pathway-mediated pyroptosis. Cell Death Discovery. 2021; 7: 251. https://doi.org/10.1038/s41420-021-00648-0.

[23] Lee EH, Park JY, Kwon HJ, Han PL. Repeated exposure with short-term behavioral stress resolves pre-existing stress-induced depressive-like behavior in mice. Nature Communications. 2021; 12: 6682. https://doi.org/10.1038/s41467-021-26968-4.

[24] Paxinos G, Watson C. The rat brain in stereotaxic coordinates. 6th edn. Academic Press: Amsterdam. 2007.

[25] Liu J, Yi S, Shi W, Zhang G, Wang S, Qi Q, *et al*. The Pathology of Morphine-Inhibited Nerve Repair and Morphine-Induced Nerve Damage Is Mediated via Endoplasmic Reticulum Stress. Frontiers in Neuroscience. 2021; 15: 618190. https://doi.org/10.3389/fnins.2021.618190.

[26] Zhang S, Li Y, Zhu W, Zhang L, Lei L, Tian X, *et al*. Endoplasmic reticulum stress induced by turbulence of mitochondrial fusion and fission was involved in stressed cardiomyocyte injury. Journal of Cellular and Molecular Medicine. 2023; 27: 3313–3325. https://doi.org/10.1111/jcmm.17901.

[27] Chiba S, Numakawa T, Ninomiya M, Richards MC, Wakabayashi C, Kunugi H. Chronic restraint stress causes anxiety- and depression-like behaviors, downregulates glucocorticoid receptor expression, and attenuates glutamate release induced by brain-derived neurotrophic factor in the prefrontal cortex. Progress in Neuro-psychopharmacology & Biological Psychiatry. 2012; 39: 112–119. https://doi.org/10.1016/j.pnpbp.2012.05.018.

[28] Romeo RD, Mueller A, Sisti HM, Ogawa S, McEwen BS, Brake WG. Anxiety and fear behaviors in adult male and female C57BL/6 mice are modulated by maternal separation. Hormones and Behavior. 2003; 43: 561–567. https://doi.org/10.1016/s0018-506x(03)00063-1.

[29] Micale V, Drago F. Endocannabinoid system, stress and HPA axis. European Journal of Pharmacology. 2018; 834: 230–239. https://doi.org/10.1016/j.ejphar.2018.07.039.

[30] Joseph DN, Whirledge S. Stress and the HPA Axis: Balancing Homeostasis and Fertility. International Journal of Molecular Sciences. 2017; 18: 2224. https://doi.org/10.3390/ijms18102224.

[31] Jones BJ, Tan T, Bloom SR. Minireview: Glucagon in stress and energy homeostasis. Endocrinology. 2012; 153: 1049–1054. https://doi.org/10.1210/en.2011-1979.

[32] Lazaroni TLN, Raslan ACS, Fontes WRP, de Oliveira ML, Bader M, Alenina N, *et al*. Angiotensin-(1-7)/Mas axis integrity is required for the expression of object recognition memory. Neurobiology of Learning and Memory. 2012; 97: 113–123. https://doi.org/10.1016/j.nlm.2011.10.003.

[33] Xie W, Zhu D, Ji L, Tian M, Xu C, Shi J. Angiotensin-(1-7) improves cognitive function in rats with chronic cerebral hypoperfusion. Brain Research. 2014; 1573: 44–53. https://doi.org/10.1016/j.brainres.2014.05.019.

[34] Marin MF, Lord C, Andrews J, Juster RP, Sindi S, Arsenault-Lapierre G, *et al*. Chronic stress, cognitive functioning and mental health. Neurobiology of Learning and Memory. 2011; 96: 583–595. https://doi.org/10.1016/j.nlm.2011.02.016.

[35] Pepys MB, Hirschfield GM. C-reactive protein: a critical update. The Journal of clinical investigation. 2003; 111: 1805–1812 [published correction appears in The Journal of clinical investigation. 2003; 112: 299]. https://doi.org/10.1172/JCI18921.

[36] Johnson TV, Abbasi A, Master VA. Systematic review of the evidence of a relationship between chronic psychosocial stress and C-reactive protein. Molecular Diagnosis & Therapy. 2013; 17: 147–164. https://doi.org/10.1007/s40291-013-0026-7.

[37] Xu J, Tang S, Song E, Yin B, Wu D, Bao E. Hsp70 expression induced by Co-Enzyme Q10 protected chicken myocardial cells from damage and apoptosis under in vitro heat stress. Poultry Science. 2017; 96: 1426–1437. https://doi.org/10.3382/ps/pew402.

[38] Kose S, Imamoto N. Nucleocytoplasmic transport under stress conditions and its role in HSP70 chaperone systems. Biochimica et Biophysica Acta. 2014; 1840: 2953–2960. https://doi.org/10.1016/j.bbagen.2014.04.022.

[39] Rogers C, Erkes DA, Nardone A, Aplin AE, Fernandes-Alnemri T, Alnemri ES. Gasdermin pores permeabilize mitochondria to augment caspase-3 activation during apoptosis and inflammasome activation. Nature Communications. 2019; 10: 1689. https://doi.org/10.1038/s41467-019-09397-2.

[40] Sorrells SF, Caso JR, Munhoz CD, Sapolsky RM. The stressed CNS: when glucocorticoids aggravate inflammation. Neuron. 2009; 64: 33–39. https://doi.org/10.1016/j.neuron.2009.09.032.

[41] Li Z, Guo J, Bi L. Role of the NLRP3 inflammasome in autoimmune diseases. Biomedicine & Pharmacotherapy = Biomedecine & Pharmacotherapie. 2020; 130: 110542. https://doi.org/10.1016/j.biopha.2020.110542.

[42] Burdette BE, Esparza AN, Zhu H, Wang S. Gasdermin D in pyroptosis. Acta Pharmaceutica Sinica. B. 2021; 11: 2768–2782. https://doi.org/10.1016/j.apsb.2021.02.006.